E-Space

Steven Bevacqua, EE, Spencer Pietryka, EE, Jonathan Scharf, EE

***Abstract*—The current implementation of wireless power transfer uses inductive power transfer, involving strongly coupled coils and high efficiency, close range transfer. This technology only works with ranges less than a few centimeters, and the coils must be orientated correctly to affect efficient power transfer. A different technology known as Magnetic Resonant Power Transfer has emerged that promises mid range, yet still high efficiency power transfer. The transmitting and receiving coils are loosely coupled, meaning the distance between them and their relative orientation is much more flexible, but resonate at a fixed frequency that still facilitates efficient transfer between them. Using this technology we are implementing a wireless power transfer system to charge a wireless phone at farther ranges than is possible with inductive technology.**

I. Introduction

Since the 1970's, transistor count and computing speed has followed Moore's law, doubling every 18 months. However in that time, battery technology has lagged far behind, with energy density only doubling between 1980 and 2010 [1]. This and the proliferation of devices including smartphones, tablets, and laptops, has led to a major problem in keeping devices charged while living an increasingly mobile life. Public locations like airports, parks, and college campuses include built-in charging stations for mobile devices or banks of outlets in their designs. The need for charging cables and ports is also an inherent weakness in electronics design. The internal electronics must be open and exposed to allow charging cables to connect. These ports put a limitation of how shock, dust, and waterproof devices can be.

However, what if devices could charge automatically without a need for ports or charging cables? This possibility has been explored with inductive charging pads. Inductive chargers offer high efficiency, but the transmitting and receiving coils need to be equally sized and oriented such that all the magnetic flux transmitted must be received. Such pads solve the problem of relying on cables and connectors, but the limited range of only a few centimeters and stringent orientation requirements mean that this technology can only be used while the device is stationary and thus batteries still need to be large and abundant.

J. D. Scharf from Plainview, NY (e-mail: jdscharf@umass.edu).
S. Pietryka from Sandwich, MA (e-mail: srpietry@umass.edu).
S. Bevacqua from Falmouth, MA (e-mail: sbevacqu@umass.edu).

Magnetic Resonant Coils offer a mid range, yet still efficient solution to this problem. The transmitting and receiving coils resonate at a fixed frequency, resulting in a high quality factor. This quality factor makes up for the fact that the coils have a lower coupling factor due to increased ranges and non-ideal relative coil orientations. The resonant fields can also charge multiple devices at once without requiring direct line of sight to the receiving devices. Ranges of two meters have been successfully demonstrated, meaning this technology could in the future be used to directly power devices or charge devices as one moves around, resulting in a diminished need for batteries [2].

This technology has important applications other than consumer electronics. This technology could revolutionize medical implants since the devices could be charged wirelessly from outside the body, instead of requiring invasive surgeries to replace batteries. It also has applications in the transportation industry as electric vehicles become more popular. Charging coils can be embedded in parking lots, bus stops, and even the road to charge vehicles at all times, effectively increasing the range and up-time of these vehicles. Since this technology is still primarily a research topic, the modest application of charging a mobile phone was chosen. The solution will involve a transmitter that will be mounted to the bottom of a desk and will be able to supply power to the receiving coil, located in a phone case, 0.25 m above the desk and 0.25 m below the desk. The iPhone 4 will be utilized, placing a limit on the size of the receiving coil to a maximum of 10.5 cm by 5.86 cm. The transmitting coil has no size restrictions. The input power will be limited by the standard wall output of 120 VAC at 60 Hz. The maximum allowed electric and magnetic fields are determined by the IEEE health regulations [3]. The specifications are listed in Table 1.

Table 1: Specifications	
System Input	120 VAC at 60Hz
Resonant Frequency	6.78 MHz
Distance/Range of Energy Transfer	0.25m
Minimum Output Power at Receiver	2.5W
Minimum Wireless Transfer Efficiency	≥40%
Minimum Total System Efficiency	≥10%
Maximum Transmitted Electric Field	121.5 V/m
Maximum Transmitted Magnetic Field	2.40 A/m

II. Design

A. Overview

The design for the magnetic resonant wireless phone charger can be broken into two main blocks with several subsystems each, which are illustrated in the block diagram below in Figure 1. The first major subsystem is the transmitter that consists of a power supply, an oscillator, control circuitry, impedance matching network, and a resonant coil. The transmitter coil and circuitry will be enclosed within a plastic case that can be attached underneath a desk or any other location desired by the user. The receiver consists of a resonant coil, an impedance matching network, a rectifier, and a DC/DC converter. A phone case will be 3D printed and the receiver coil and circuitry will be placed inside. A small USB cable will then connect the phone to the output of the DC/DC converter to charge the phone. Additionally, there is also the option to include a repeater located at some point between the transmitter and receiver. A repeater is another coil that is tuned to the same resonant frequency as the transmitter and receiver coils, which can help to improve distance and efficiency of the power transfer [4].

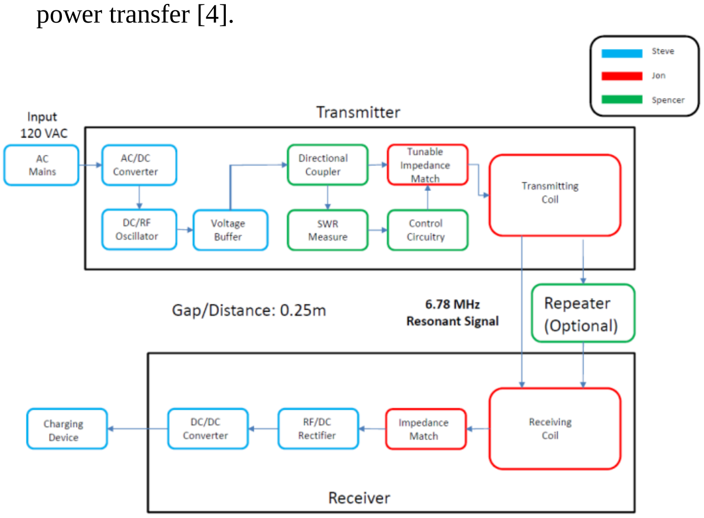

Figure 1. Block Diagram

The block diagram shows the subsections of the two major blocks used for the phone charger as well as division of labor among the team. The following descriptions outline each subsection as well as the technology used to create and test them before implementation.

B. Power Supply

A power supply or AC/DC converter is the first step in the block diagram because it is used to source the power for transmission between the coils as well as supplying power for the other circuits in the transmitter. AC power directly from the wall operates around 50-60 Hz, which is much lower than the resonant frequency of the coils. Instead of directly converting the frequency from 60 Hz to 6.78 MHz, the AC wall power will be converted to DC with the power supply and then used to power the oscillator at the resonant frequency of the coils. Additionally, the converted DC power is to be used to supply operating voltages for integrated circuits and other components that make up the transmitter circuitry. To meet the 10 percent efficiency specification at the maximum distance while supplying 2.5 W to the phone, the required power supply will need to be able to source at least ten times the output power. Therefore, around a 25 W or greater power supply or AC/DC converter will be required.

C. Oscillator

Nearly every circuit contains an oscillator of some type to control the frequency of operation. In this case, the oscillator will be used to set the operating frequency to the resonant frequency of the transmitter and receiver coils. There are a wide variety of oscillators that can produce frequencies in the megahertz range, but one used in this design is the Colpitts oscillator [2]. The Colpitts oscillator is an LC oscillator, so the reasoning in selecting it is that the transmitter coil could be used as the inductor of the oscillator and could eliminate the need for other stages between the oscillator and coil. Using an oscilloscope, a frequency of 6.78 MHz was achieved. Although the oscillator design was able to produce the correct resonant frequency, the frequency would shift very easily as the distance between the transmitter and receiver coils varied. This resulted in different loads on the oscillator with undesirable frequency changes, which is especially detrimental in a frequency sensitive application where a tight bandwidth around the resonant frequency is required. Therefore, a new oscillator using a quartz crystal will be designed using a different topology than the Colpitts oscillator. The frequency from a quartz crystal oscillator is typically very stable compared to an LC oscillator where capacitors can have tolerances of around 20 percent that directly alter the frequency. The design can first be simulated using SPICE and then built in the lab. By using an oscilloscope, the frequency of the oscillator can be measured as a test. The oscillator schematic is shown in Figure 2.

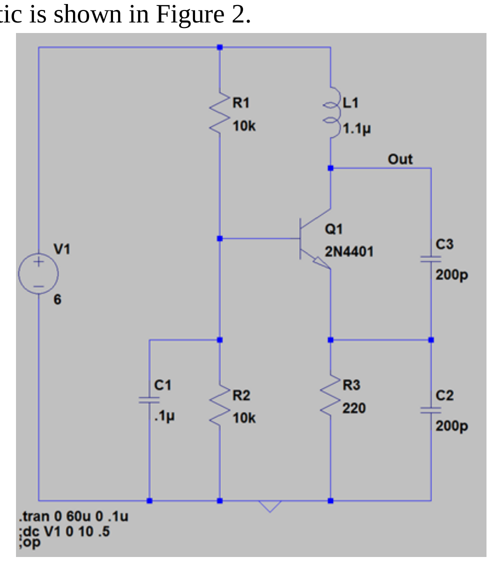

Figure 2. Colpitts Oscillator

D. Voltage Buffer

As mentioned in above in the oscillator section, operating at the resonant frequency is crucial for the technology to efficiently work. By loading the output of the oscillator, the frequency can shift away from resonance. To prevent this from happening, a voltage buffer is placed at the output of the oscillator. The current application uses a source follower topology for a voltage buffer. A high input impedance and low output impedance help to isolate the oscillator from loading by the coil and other transmitter subsections. The voltage buffer also has a voltage gain close to one and an ideally infinite current gain. By increasing the current going to the coil, the magnetic field of the transmitter coil will be larger that helps obtain greater distance in power transfer. The first design was a source follower using an IRF540 NMOS [5] transistor with a constant current source using an LM317 [6] voltage regulator. A sinusoid enters the NMOS gate and the output is on the source of the NMOS, where the transmitter coil is located. After trial and error, the LM317 was found not to operate up to 6.78 MHz accurately. A BJT constant current source then replaced the voltage regulator constant current source using a 2N3053 NPN. The voltage buffer was tested using a function generator at the input and connecting the transmitter coil with a one ohm resistor on the output. The current through the one ohm resistor was measured and compared to the SPICE simulation to ensure proper operation. The voltage buffer schematic is in Figure 3.

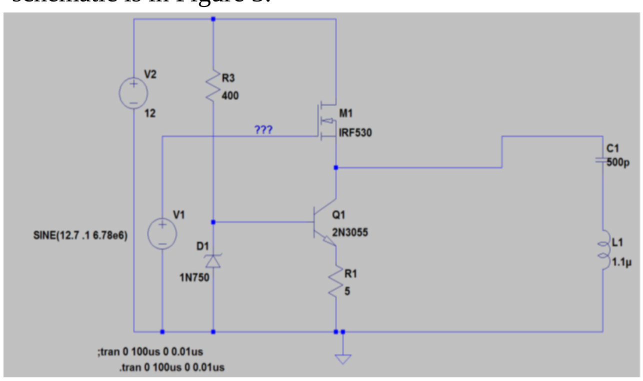

Figure 3. Voltage Buffer

E. Directional Coupler

The directional coupler will facilitate measuring the voltage of the incident and the reflected wave on the line, ultimately giving a way to quantify load mismatch and tune the impedance matching network to achieve maximum power transfer from the source to the transmitting coil. Building of this block will require a coupler capable of handling the power requirements of our design, while still providing good directionality. Knowledge of microwaves will aid in the design of this block. It can be tested by using a signal generator to provide a known input signal while terminating the output of the directional coupler with a known load. Utilizing the Microwave Instructional Laboratory, a power meter can be used to measure the power of the coupled outputs to verify they are providing the correct outputs.

F. SWR Measure

The SWR Measure block will use the coupled outputs of the directional coupler as its inputs. The MAX2016 IC made by Maxim Integrated can use these inputs to determine a VSWR (voltage standing wave ratio) [8]. This VSWR can be tested by terminating the directional coupler in a known load and calculating the reflection coefficient and subsequently the VSWR and comparing that to the output of the Maxim Integrated IC.

G. Control Circuitry

The control circuitry will consist of an analog to digital converter, a microcontroller, and a digital to analog converter that will provide the voltage to set the voltage variable capacitors in the tunable impedance matching network. The inputs of this block will be the VSWR measure from the SWR Measure block and the output will be fed to the tunable impedance matching network. This block will primarily involve coding the microcontroller with algorithms that will take the VSWR measure, and convert that into a return loss measure. The capacitor values in the impedance matching network can then be calculated from the return loss. It can be tested by feeding the microcontroller set inputs and ensuring that the algorithms are correctly calculating the capacitor values.

H. Impedance Matching Networks

Magnetic wireless resonant power transfer involves creating an LC resonance, and transferring power via electromagnetic coupling. As a result, the magnetic coupling can be illustrated by the mutual inductance, L_m, shown in Figure 4 [9], where Z_{source} is the characteristic impedance, Z_{load} is the impedance of the load, and the ohm loss due to radiation is represented by R.

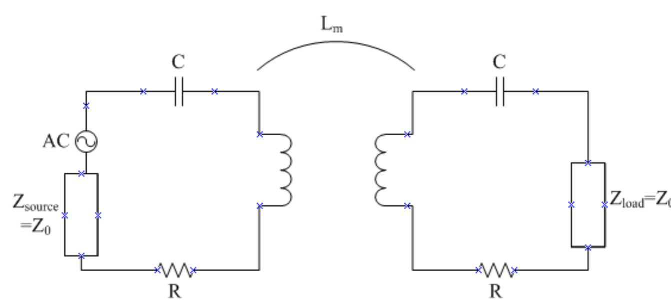

Figure 4. Transmitter and Receiver Schematic

In order to achieve efficient wireless resonant power transfer for our system, both the transmitter and the receiver coils need to be operating at resonant frequency. From this typology, the resonance frequency can be calculated based on the following component values. In order to satisfy the resonance condition the reactance must be zero as shown in equation (1) below. Following this the two resonant frequencies for both the transmitter and receiver can be calculated from equations (2) and (3). Next, the two resonant frequencies can be used to calculate the coupling coefficient shown in equation (4).

$$\omega_m = \frac{\omega_0}{\sqrt{(1+k)}} = \frac{1}{\sqrt{(L+L_m)C}} \quad (1)$$

$$\omega_m = \frac{\omega_0}{\sqrt{(1+k)}} = \frac{1}{\sqrt{(L+L_m)C}} \quad (2)$$

$$\omega_e = \frac{\omega_0}{\sqrt{(1-k)}} = \frac{1}{\sqrt{(L-L_m)C}} \quad (3)$$

$$k = \frac{L_m}{L} = \frac{\omega_e^2 - \omega_m^2}{\omega_e^2 + \omega_m^2} \quad (4)$$

However, as the distance between the coils increases, the coupling between the two coils weakens and the coupling coefficient that ensures efficient power transfer reduces. As a result, the impedance for both the transmitter and receiver circuits will change due to the change in the coupling coefficient, and the effective resonance frequency will change as well. Article **[9]** shows how the coupling factor reduces with increasing distance [Figure 5] for two 5 turn 150mm radius, 5mm pitch helical coils.

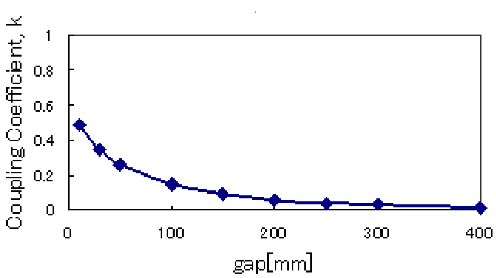

Figure 5. Coupling Factor vs. Distance between Coils

As a result, the efficiency vs. frequency for increasing distances can be seen in Figure 6 from article [9**]**, where the pink curves represent the power efficiency of reflection and the blue curve represents the power efficiency of transmission.

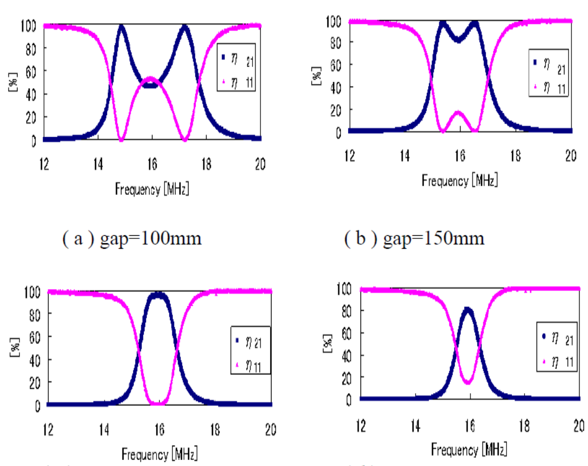

(a) gap=100mm (b) gap=150mm

(c) gap=200mm (d) gap=250mm

Figure 6. Efficiency vs. Frequency at Various Gap Distances

From the figure one can see that at a shorter distance of about 100 mm, there are two twin peaks in efficiency but as the distance increases these frequencies converge at a midpoint and eventually reduces in amplitude.

Due to the change in resonant frequency with distance, prior research has demonstrated wideband frequency tuning techniques that can automatically change the operating frequency to the resonant frequency at various distances to ensure optimum efficiency. However, due the Industrial-Scientific-Medical (ISM) band regulations, there are only certain frequencies allocated with a limited bandwidth available for purposes other than for communication. In the Code of Federal Regulations, Tile 47, Part 15, available operating frequencies are specified in Table II with the corresponding bandwidths. From the Figure 7 [10], it is illustrated that at lower frequencies there is considerable power loss, and at higher frequencies beyond 20 megahertz, there arises major design problems due to cost, size, and power allocation for certain components. As a result, it was found that the best operational frequency is a stable 6.78 megahertz, which has a practical bandwidth of 15 kilohertz.

ISM frequency	Tolerance
6.78 MHz	±15.0 kHz
13.56 MHz	±7.0 kHz
27.12 MHz	±163.0 kHz
40.68 MHz	±20.0 kHz
915 MHz	±13.0 MHz
2,450 MHz	±50.0 MHz
5,800 MHz	±75.0 MHz
24,125 MHz	±125.0 MHz
61.25 GHz	±250.0 MHz
122.50 GHz	±500.0 MHz
245.00 GHz	±1.0 GHz

Table II. Code of Federal Regulations, Tile 47, Part 15 Available ISM Band Frequencies

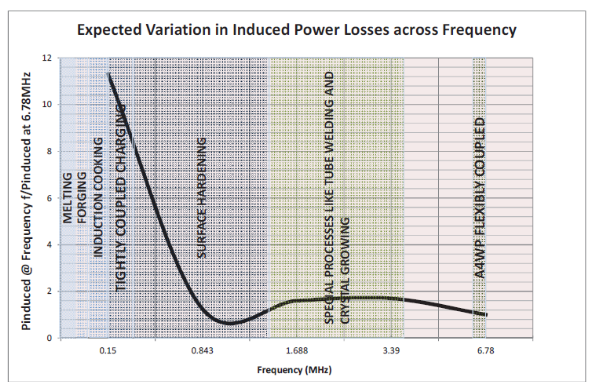

Figure 7. Power Loss vs. Operational Frequency

Therefore, in order to ensure that we are performing at resonant frequency without violating ISM band regulations and changing our operational frequency, impedance matching can be used to obtain the optimum wireless power transfer efficiencies at various distances. From article [9], Figure 8a illustrates that at their operating frequency of 13.56 megahertz, before impedance matching that obtained about a 50% efficiency wireless power transfer. However, Figure 8b shows that after impedance matching, they were able to operate at resonant frequency obtaining a wireless power transfer efficiency of 90%.

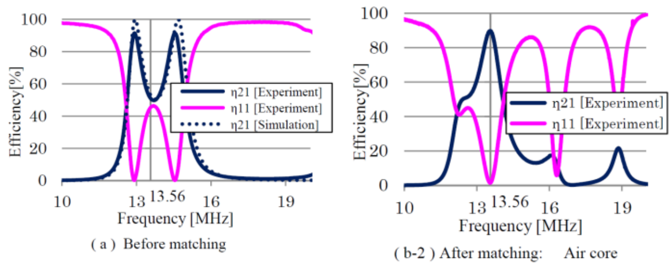

Figure 8. Efficiency vs. Frequency After and Before Impedance Matching

In developing an impedance matching network suitable for achieving optimum efficiency, it is found that a pi-model typology is strongly preferred over other types of networks, Figure 9 [11]. Unlike an L-model typology, a pi-model typology enables wideband impedance matching to load impedances that are greater than, equal to, or less than the source impedance. Additionally, since the impedance will need to change with distance, it allows for a fixed inductor value to be placed in the high-current path, and variable source and load capacitor values to tune and control the impedance matching. From the equations below, the capacitor values for C_S and C_L can be calculated to ensure a high quality factor, Q_m, and optimized to those values by implementing voltage-varying capacitors. To test that the correct values are being used, one can use a Network Analyzer to ensure the impedance matching network is working correctly and providing the most optimum power transfer efficiency.

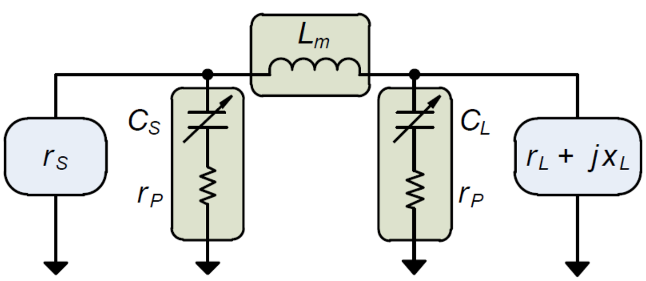

$$\left.\begin{aligned} Q_m &= \sqrt{-1 + \frac{r_l(r_l + r_s)}{L_m^2 w_0^2} + \frac{2r_l\sqrt{r_l r_s - L_m^2 w_0^2}}{L_m^2 w_0^2}} \\ C_S &= \frac{\sqrt{-1 + \frac{(1+Q_m^2)r_s}{r_l}}}{r_s w_0} \\ C_L &= \frac{Q_m}{r_l w_0} \end{aligned}\right\} r_s < r_L$$

Figure 9. Schematic and Equations in Pi-Model Impedance Matching Network for Wireless Resonant Power Transfer

I. Transmitter and Receiver Coils

In designing the transmitter and receiver coils, the most important consideration is the quality factor, Q. The quality factor of the resonant coils is a measure of how well the coils store and dissipate energy. Essentially, the higher the quality factor, the more efficient the coils are in storing energy.

Calculating the quality factor is illustrated in Figure 10 [2]. From the quality factor, the figure of merit, U, can be determined. Accordingly, by assuming an optimum impedance matching network, the optimum power efficiency vs. figure of merit is illustrated in Figure 10, and the relationship shows that a large figure of merit will lead to a more efficient power transfer. Since the figure of merit is determined by the coupling coefficient and the quality factor of the two coils, increasing the quality factor will increase the optimum wireless transfer efficiency.

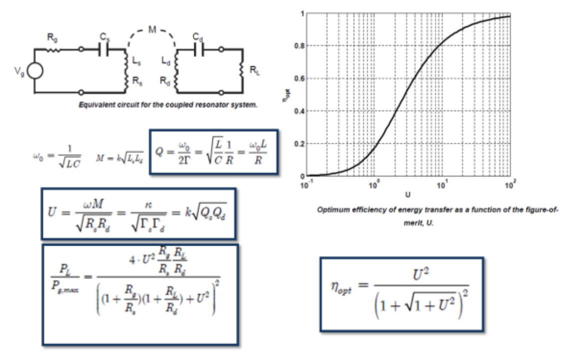

Figure 10. Quality Factor and Figure of Merit Calculations

The quality factor is dependent on the angular frequency, inductance, and resistance. Since the frequency will be fixed at 6.78 megahertz, having the smallest coil resistance and largest inductance will lead to the highest quality factor. The inductance and resistance of a coil can be calculated from the equations in Figure 11 [12]. The equations show that the inductance has a relationship to the number turns, N, squared, while the resistance is only linearly dependent. As a result, the Q increases linearly with the number of turns in a flat coil design.

$$L = \frac{N^2 \mu A}{l}$$

$$R = \frac{2\pi a N}{\sigma 2\pi r \delta} = \frac{aN}{\sigma r \delta}$$

Figure 11. Calculations for Inductance and Resistance for Flat Coil Design

Apart from the quality factor, the ratio of the coil sizes also considerably affects the wireless transfer efficiency. Figure 12 illustrates that as the distance in relation to the transmitting coil diameter increases, different coil ratios will lead to different efficiencies [13]. For instance, when the ratio of the receiver coil diameter to the transmitter coil is 1, the maximum wireless transfer efficiency is observed. However, the smaller ratio becomes, the quicker the efficiency tends to drop off. At about a ratio of .3, the efficiency is about 60% at 1 transmitter coil length. As a result, in order to meet wireless power transfer efficiency above 40% at a coil length distance, a ratio above about .3 should be used.

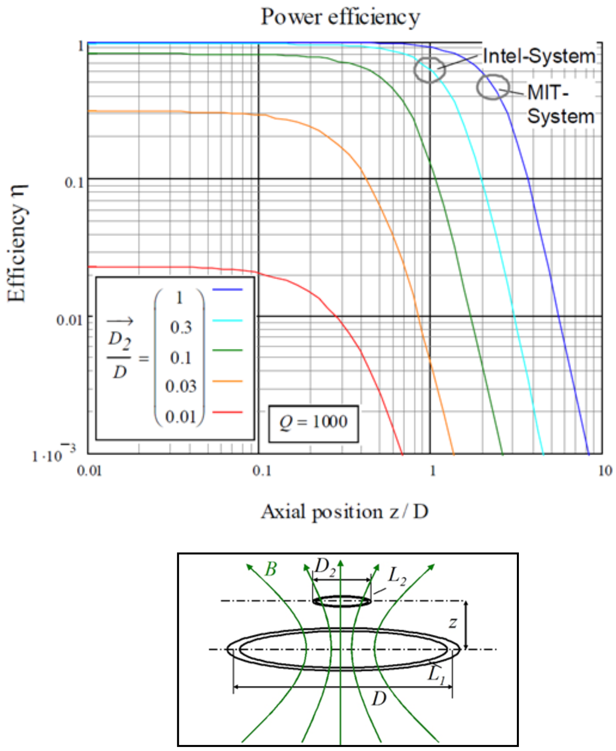

Figure 12. Plot When Quality Factor is 1000 of Different Ratios at of Receiver Coil Diameter to Transmitter Coil Diameter in Efficiency vs. Distance per Receiver Coil

In Figure 12, the Q factor for the two coils is 1000. However, if this coil factor were to increase, the efficiency drop would extend beyond what is shown in the diagram. In other words, the higher the Q factor, the smaller the ratio can be made for the same amount efficiency.

In designing the coils, a multi-turn transmitter and receiver typology should be implemented with the largest wire thickness possible for the fitted area to obtain a smaller resistance. Additionally, a receiver to transmitter diameter coil ratio should be greater than .3 to ensure that the efficiency doesn't drop off considerably at shorter distances. To test the quality factor of the coils, an LCR parameter analyzer will be used, and the effective power efficiency will be measured using an oscilloscope.

J. *RF/DC Rectifier*

A rectifier is important in the receiver section because it converts the received signal at 6.78 MHz back to a DC voltage that can be utilized by electronics, such as a phone. The rectifier will be purchased as an IC so that it is compact and inexpensive. To test the rectifier, an AC signal such as a sinusoid from the function generator will be put to it and the output will be measured with a multimeter or oscilloscope to view the DC voltage. Additionally, an LED or other low power device could be put on the output to see if it works accurately after first testing it with the function generator.

K. *DC/DC Converter*

While the output of the RF/DC regulator is a DC voltage that could be an input to the phone or charging device, it may exceed the accepted range of the device. This could potentially not charge the device or even damage it. Typically for USB charging, the output voltage is 5V and about 500mA to 1.2A depending on the charger. Therefore, a DC/DC converter or regulator is necessary to keep a constant output of about 5V to the phone. Additionally, the regulator must be able to source enough current otherwise the power requirements may not be met, preventing the phone from charging at all. A DC/DC regulator with the desired specifications range of input and output voltages and currents will be purchased in an IC package if possible. To test that it works, the nominal input voltage will be provided from a power supply and the output voltage will be measured to ensure proper operation. After this is verified, it can be connected to the output of the rectifier and the two can be tested together.

III. Project Management

The primary goal of MDR was to illuminate an LED from half a meter away using magnetic resonance technology. To do this, the resonant transmitter and receiver coils were constructed as well as a voltage buffer that received a sinusoid from the signal generator as an input instead of using the oscillator. The block diagram of the MDR demonstration is shown in Figure 13. Using the circuit from the block diagram, all of the MDR goals were met. The LED could be illuminated from up to and beyond the half meter distance that was specified originally.

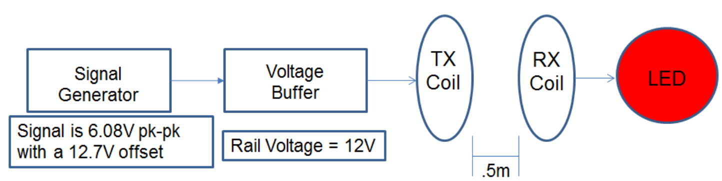

Figure 13. MDR Block Diagram

Overall, the team is functioning very well together and has had no major issues regarding communication or work distribution. Each group member is like-minded in that they are willing to dedicate more time to the project in order to learn about magnetic resonant charging and deliver the final project in the spring. Additionally, each group member has certain areas of expertise that prove useful to different aspects of the project. Each member has the same electrical engineering background from the same course work over the past several years, but further expertise and specialization have resulted from summer research and internship experience. Spencer has had experience working for a microwave engineering company, and therefore has more experience with equipment and high frequency measurements that enable him to design the control circuitry with the directional coupler for SWR measurement. Jon has had experience performing research with UMass electrical engineering professors that have required him to design impedance matching networks and PCBs, which qualifies him to design the impedance matching network for the transmitter and receiver. Steven has had experience building prototypes of circuits from internships and is currently enrolled in the Analog IC course which utilizes MOSFET technology that can relate to designs for this project. He has experience soldering and crimping as well, which can help with the final assembly of the project. Each team member is very supportive of each other. If anyone has a question on a concept from a research paper or needs help constructing a circuit, everyone is willing to help the other person. The group communicates on a close to daily basis and officially meets twice a week for project work. A Gantt chart in Figure 14 shows the work done by each team member and the work looking ahead.

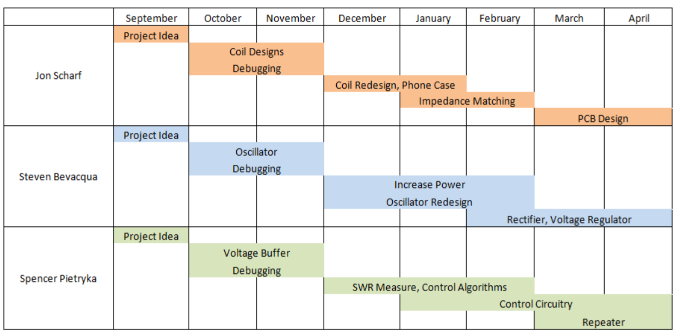

Figure 14. Gantt Chart

IV. Conclusion

Currently, a signal generator is being utilized to create the 6.78 MHz signal that acts as the input to the voltage buffer. A Colpitts oscillator has been constructed that oscillates at the correct frequency when unloaded, but the gate capacitance of the voltage regulator causes instabilities that limit its use. A plan to switch over to a quartz oscillator that is more stable should solve this problem. The voltage buffer is working at this stage and looking forward it just needs to be constructed with more robust components to handle the greater power demands of the mobile device. The coils have been constructed and demonstrate a high Q factor. They will need to be re-sized for the final implementation. The control circuitry, impedance matching, AC/DC rectifier, and DC/DC converter at the receiver need to be designed and constructed. The largest obstacles looking forward will be matching the impedance of the voltage buffer to the very low impedance of the resonant coils and obtaining parts capable of handling the power requirements of the mobile device on a limited budget.

References

[1] C. X. Zu and H. Li, “Thermodynamic analysis on energy densities of batteries,” Energy Environ. Sci., 2011, vol. 4, pp. 2614-2624

[2] M. Kesler, "Highly resonant wireless power transfer: safe, efficient, and over distance.", WiTricity Corporation. 2013.

[3] “IEEE Standard for Safety Levels with Respect to Human Exposure to Radio Frequency Electromagnetic Fields, 3 kHz to 300 GHz”, IEEE Std. C95.1-2005.

[4] Dukju Ahn; Songcheol Hong, "A Study on Magnetic Field Repeater in Wireless Power Transfer," in Industrial Electronics, IEEE Transactions on , vol.60, no.1, pp.360-371, Jan. 2013

[5] Vishay Siliconix, “Power MOSFET,” IRF540 datasheet, Mar. 2011.

[6] Texas Instruments, “LM317 3-Terminal Adjustable Regulator,” LM317 datasheet, Sept. 2006 [Revised Oct. 2014].

[7] Central Semiconductor Corp. “Silicon NPN Transistors,” 2N3053 datasheet, Dec. 2013.

[8] Maxim Integrated, “LF-to-2.5GHz Dual Logarithmic Detector/ Controller for Power, Gain, and VSWR Measurements,” MAX2016 datasheet, 2006.

[9] Teck Chuan Beh; Imura, T.; Kato, M.; Hori, Y., "Basic study of improving efficiency of wireless power transfer via magnetic resonance coupling based on impedance matching," in Industrial Electronics (ISIE), 2010 IEEE International Symposium on , vol., no., pp.2011-2016, 4-7 July 2010

[10] Tseng, R.; von Novak, B.; Shevde, S.; Grajski, K.A., "Introduction to the alliance for wireless power loosely-coupled wireless power transfer system specification version 1.0," in Wireless Power Transfer (WPT), 2013 IEEE , vol., no., pp.79-83, 15-16 May 2013

[11] Waters, Benjamin H., Alanson P. Sample, and Joshua R. Smith. "Adaptive impedance matching for magnetically coupled resonators." PIERS Proc(2012): 694-701.

[12] Cannon, B.L.; Hoburg, J.F.; Stancil, D.D.; Goldstein, S.C., "Magnetic Resonant Coupling As a Potential Means for Wireless Power Transfer to Multiple Small Receivers," in Power Electronics, IEEE Transactions on , vol.24, no.7, pp.1819-1825, July 2009

[13] Waters, Benjamin H., Alanson P. Sample, and Joshua R. Smith. "Adaptive impedance matching for magnetically coupled resonators." PIERS Proc(2012): 694-701.